

Enzymes

Deutsche Ausgabe: DOI: 10.1002/ange.201605232
 Internationale Ausgabe: DOI: 10.1002/anie.201605232

Structure and Mechanism of the Sphingopyxin I Lasso Peptide Isopeptidase

Christopher D. Fage⁺, Julian D. Hegemann⁺, Annika J. Nebel, Roman M. Steinbach, Shaozhou Zhu, Uwe Linne, Klaus Harms, Gert Bange, and Mohamed A. Marahiel*

Abstract: Lasso peptides are natural products that assume a unique lariat knot topology. Lasso peptide isopeptidases (IsoPs) eliminate this topology through isopeptide bond cleavage. To probe how these enzymes distinguish between substrates and hydrolyze only isopeptide bonds, we examined the structure and mechanism of a previously uncharacterized IsoP from the proteobacterium *Sphingopyxis alaskensis* RB2256 (SpI-IsoP). We demonstrate that SpI-IsoP efficiently and specifically linearizes the lasso peptide sphingopyxin I (SpI) and variants thereof. We also present crystal structures of SpI and SpI-IsoP, revealing a threaded topology for the former and a prolyl oligopeptidase (POP)-like fold for the latter. Subsequent structure-guided mutational analysis allowed us to propose roles for active-site residues. Our study sheds light on lasso peptide catabolism and expands the engineering potential of these fascinating molecules.

Lasso peptides are an emerging class of natural products^[1] belonging to the ribosomally synthesized and post-translationally modified peptide (RiPP) family. They are distinguished by their unusual lariat knot topology: the C-terminal tail is threaded through a 7–9-residue macrolactam ring bearing an isopeptide bond between the N-terminal α -amino group and the side chain of an acidic residue. This strained conformation is secured through the placement of bulky side chains (plugs) on either side of the ring and endows the molecule with resistance to chemical, proteolytic, and (often) thermal degradation.^[1a,2] Due to their inherent stability, sequence malleability, and low toxicity, lasso peptides may be employed as scaffolds for bioactive epitope grafting.^[3] They also possess a variety of biologically relevant activities, serving as antimicrobials, enzyme inhibitors, and receptor antagonists.^[1,3,4]

Like all RiPPs, lasso peptides are first ribosomally synthesized as a precursor peptide (protein A), which is then processed into its mature form by enzymes (proteins B and C) encoded within the biosynthetic gene cluster (Figure S1 in the Supporting Information).^[1,5] Some clusters also

harbor a downstream gene coding for an ATP-binding cassette (ABC) transporter (protein D) for efflux of the lasso peptide from the cell, thus conferring self-immunity.^[1,2,6]

In recent years, a large number of new proteobacterial lasso peptides that evidently lack antimicrobial activity have been isolated by genome-mining approaches.^[2b,6a,7] Most of these gene clusters do not encode a dedicated ABC transporter. Instead, they neighbor a highly conserved cluster coding for a prolyl oligopeptidase (POP) homologue,^[8] as well as a TonB-dependent receptor and σ /anti- σ factors homologous to siderophore import and regulation machinery, respectively (Figure 1a).^[1,2b,6a,7a,c] Investigation of the POP

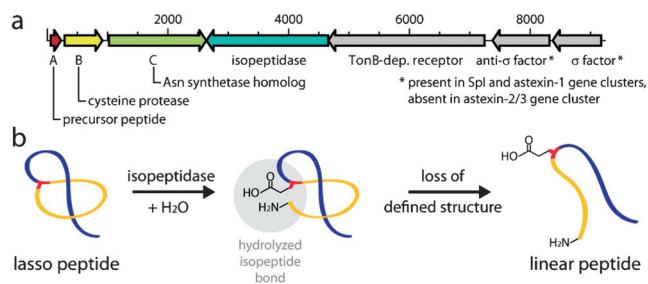


Figure 1. a) Typical arrangement of lasso peptide biosynthesis and IsoP-encoding gene clusters. b) IsoP-catalyzed hydrolysis.

homologues AtxE1 and AtxE2 from *Asticcacaulis excentricus* CB48 led to the discovery of IsoP activity toward the lasso peptides astexin-1 and astexin-2/3, respectively, with no apparent cross-reactivity (Figure 1b).^[2b] The lariat topology was shown to be essential for hydrolysis, since AtxE2 failed to linearize a branched-cyclic isomer of astexin-2 in vitro. Additionally, AtxE2 cleaved astexin-2/3 loop variants to a lesser extent than the wildtype (wt), which points to crucial recognition features in the loop region.^[9] Based on these findings, as well as the presence of putative import and regulation machineries, the IsoP-encoding operon may play a role in lasso peptide dependent signaling.^[1a] Notably, lasso peptide IsoPs are the only enzymes known to function solely in RiPP catabolism.^[9]

Specificity toward a distinct tertiary fold, as seen for AtxE2 toward astexin-2/3, contrasts with that of typical proteases, which simply cleave at a certain amino acid sequence (e.g., POPs cleave after Pro).^[2b,8] While POPs and lasso peptide IsoPs belong to the serine protease family, most other IsoPs, including ubiquitin-specific processing proteases (USPs)^[10] and sentrin/SUMO-specific proteases (SENPs),^[11] which hydrolyze Gly-Lys bonds, and transglutaminases

[*] Dr. C. D. Fage,^[+] Dr. J. D. Hegemann,^[+] A. J. Nebel, R. M. Steinbach, S. Zhu, Dr. U. Linne, Dr. K. Harms, Dr. G. Bange, Prof. Dr. M. A. Marahiel
 Fachbereich Chemie, Fachgebiet Biochemie und LOEWE-Zentrum für Synthetische Mikrobiologie, Philipps-Universität Marburg
 Hans-Meerwein-Strasse 4, 35032 Marburg (Germany)
 E-mail: marahiel@staff.uni-marburg.de

[+] These authors contributed equally to this work.

Supporting information for this article can be found under:
<http://dx.doi.org/10.1002/anie.201605232>.

(TGs),^[12] which hydrolyze ϵ -(γ -Glu)-Lys bonds, are cysteine proteases. Only the i-type lysozymes, which hydrolyze ϵ -(γ -Glu)-Lys bonds, are also serine proteases.^[13] Notably, a PubMed search reveals no other examples of IsoPs in the literature.

After reports of AtxE1 and AtxE2, we decided to investigate other examples of this intriguing family of enzymes. To this end, we cloned eight IsoP-encoding genes into pET41a and tested heterologous expression and solubility (Table S1 in the Supporting Information). Only that encoding SpI-IsoP, which is found next to the SpI biosynthetic gene cluster from *S. alaskensis* RB2256, yielded adequate amounts of soluble protein. Preliminary in vitro assays showed that 0.1 μ M SpI-IsoP completely hydrolyzes 100 μ M SpI within 5 min at 30 °C (Figures S2a and S3). Subsequent determination of kinetic parameters for the reaction of SpI-IsoP with SpI indicated that the enzyme processes its substrate significantly more efficiently than AtxE2 does (Figure 2 and Table S2).^[2b]

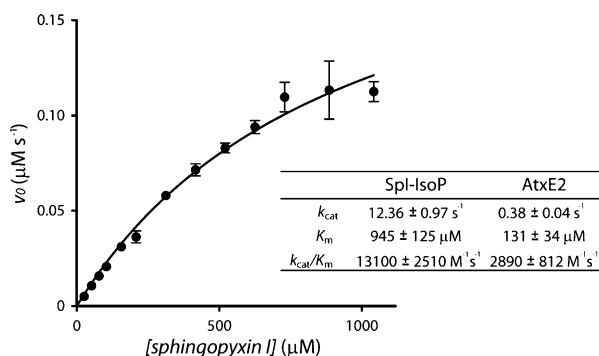


Figure 2. Michaelis–Menten kinetics of SpI-IsoP. For each concentration of SpI, v_0 was determined in triplicate (data represent mean \pm SD). The kinetics of AtxE2 were determined previously.^[2b]

To establish the substrate specificity of SpI-IsoP, the enzyme was assayed in vitro against a diverse panel of previously described lasso peptides (Figure 3).^[3,4,7,14] A branched-cyclic isomer of SpI was generated as an additional substrate through unthreading at 95 °C.^[7c] However, neither this isomer nor any of the 23 lasso peptides tested (including sphingopyxin II, which is also produced by *S. alaskensis* RB2256) were cleaved, even after 60 min. This contrasts starkly with the complete hydrolysis of threaded SpI within 5 min and indicates that SpI-IsoP shows remarkably high specificity toward its native substrate. To inspect the lasso fold of this substrate, we elucidated its crystal structure to 0.85 Å (Table S3, Figure 4a–d, and Figure S4).

Previously, AtxE2 was shown to be inactive toward astexin-1 while still recognizing astexin-2/3 variants.^[9] To investigate whether SpI-IsoP selectively recognizes the SpI fold, with relaxed specificity toward the primary structure, we generated a library of 17 SpI variants. Except for the E10A, Y16A/L17A/F18A, Y16A, H15A, and insertion variants, all compounds were produced in moderate to good yield relative to wt SpI (Figure 4d, Table S4), which is in agreement with the promiscuous nature of lasso peptide biosynthetic machin-

X1-Za XXXXXZXXXXXXXXXb HN ————— CO b = length		lasso peptide of producing strain
hydrolyzed by SpI-IsoP		not hydrolyzed by SpI-IsoP
class I		
C1-D9	CLGVGSND ³ FAGGYAIVCFW ²¹	siamycin I* of <i>Streptomyces</i> sp. SKH2344
class II		
G1-E7	GGPLAGE ¹ EIGGFNVPG ¹⁶	xanthomonin I* of <i>Xanthomonas gardneri</i> ATCC 19865
	GGPLAGE ¹ EMGGITT ¹⁴	xanthomonin II* of <i>Xanthomonas gardneri</i> ATCC 19865
	GGAGAGE ¹ VNGMSP ¹³	xanthomonin III of <i>Xanthomonas citri</i> pv. <i>magniferae</i> LM941
G1-D8	FGIGWGN ¹ IFGHYSYGF ¹⁷	anantoin of <i>Streptomyces coeruleus</i>
	FGSKPLD ¹ SFGLNFF ¹⁵	chaxapeptin* of <i>Streptomyces leeuwenhoekii</i> C58
	GPGGITG ¹ VGLGENNF ¹⁷	sphingonodin I of <i>Sphingobium japonicum</i> UT26
	GEALIDQ ¹ VGGGRQQFLT ¹⁹	sphingopyxin II of <i>Sphingopyxis alaskensis</i> RB2256
	GISGGTV ¹ DAPAGQLAG ¹⁷	syonodin I of <i>Sphingobium yanoikuyae</i> XLDN2-5
G1-E8	GGAGQYKE ¹ VEAGRWSDR ¹⁷	burhizin of <i>Burkholderia rhizoxinica</i> HK1 454
	GDVLNAP ¹ PGIGREPTG ¹⁷	caulonodin I of <i>Caulobacter</i> sp. K31
	GDVLFAP ¹ PGVGRPPMG ¹⁷	caulonodin II of <i>Caulobacter</i> sp. K31
	GQIYDHP ¹ VGIGAYGCE ¹⁷	caulonodin III of <i>Caulobacter</i> sp. K31
	GAFFVGQPE ¹ AVNPLGREIQG ¹⁹	caulosegnin I* of <i>Caulobacter segnis</i> ATCC 21756
	GGAGHVPE ¹ YFVGITPTISFYG ²¹	microcin J25* of <i>Escherichia coli</i> AY25
G1-D9	GLSQGEVPE ¹ IGQTYFEESR ¹⁹	astexin-1* of <i>Asticcacaulis excentricus</i> CB48
	GTPGFQTPD ¹ ARVISRFGN ¹⁹	capistruin* of <i>Burkholderia thailandensis</i> E264
	GIEPLGPVD ¹ EDQGEHYLFAGG ²¹	sphingopyxin I of <i>Sphingopyxis alaskensis</i> RB2256
G1-E9	GTLTPGLE ¹ DFLPGHYMPG ¹⁹	caulosegnin II* of <i>Caulobacter segnis</i> ATCC 21756
	GALVGLLE ¹ DITVARYDPM ¹⁹	caulosegnin III of <i>Caulobacter segnis</i> ATCC 21756
	GAPSLINSE ¹ DNPAFPQRV ¹⁹	rubrivinodin of <i>Rubrivivax gelatinosus</i> IL44
S1-E9	SIGDSGLRE ¹ SMSSQTYWP ¹⁸	caulonodin V* of <i>Caulobacter</i> sp. K31
A1-E9	AGTGVLLE ¹ TNQIKRYDPA ¹⁹	caulonodin VI of <i>Caulobacter</i> sp. K31
class III		
G1-D9	GLPWG ¹ PSD ¹ IPGWNTPA ¹⁹	BI-32169* of <i>Streptomyces</i> sp. DSM 14996

* three-dimensional structures published in previous literature

Figure 3. Lasso peptides tested for hydrolysis by SpI-IsoP.^[3–4,7,14]

ies.^[7a,b,d,9,14a,15] After confirming the threaded topology of the variants through a combined thermal stability/carboxypep-

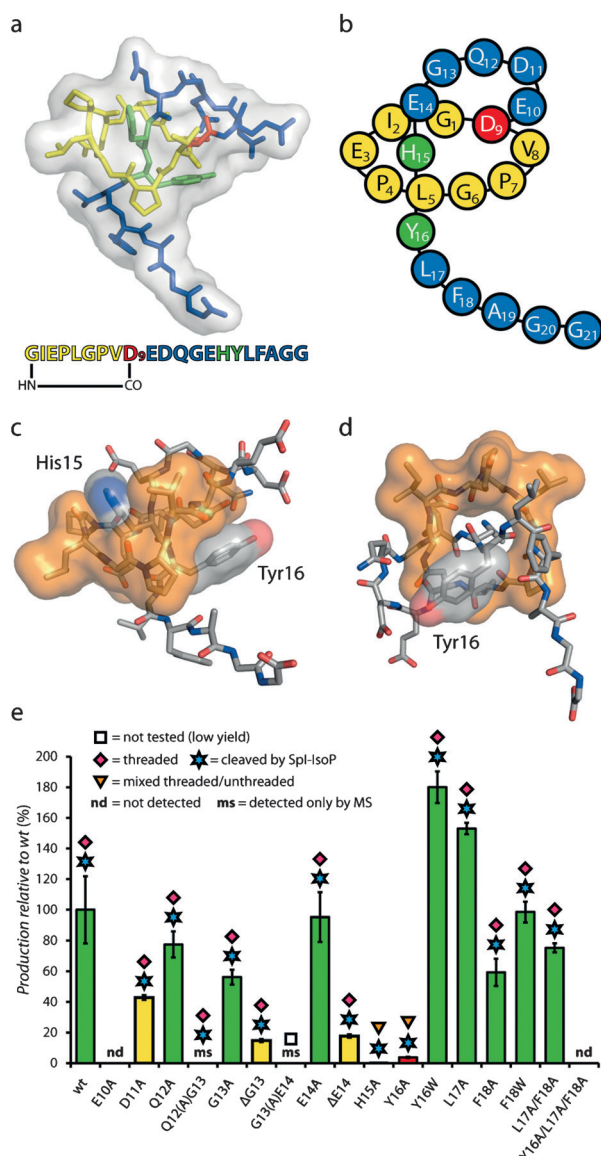


Figure 4. a) Crystal structure of Spl (PDB ID: 5JQF). The primary structure and color coding are shown below. b) A cartoon representation of Spl, colored as in (a). c, d) Two views of Spl, emphasizing the ring and plugs. e) Production and analysis of Spl variants. Each variant was tested in triplicate (data represent mean \pm SD). Bars are colored by relative production: green 50–200%, yellow 10–50%, red (0–10%).

tidase Y assay (Figure 4e, Figure S5, and Table S5), they were tested for IsoP-mediated hydrolysis. All variants were cleaved by SpI-IsoP, thus illustrating tolerance of minor differences in the loop and tail regions of the substrate, including longer or shorter loops (Figure 4e and Table S5).

To probe how SpI-IsoP modifies a single lasso peptide substrate, we solved the crystal structure of the enzyme to 3.0 Å (Table S3). Similar to POPs,^[8] the 79.4 kDa protein consists of two domains: an N-terminal β -propeller (residues 1–419) and a C-terminal α/β -hydrolase (residues 420–726; Figure 5 and Figures S6–8).

These domains envelop a voluminous cleft of approximately 12 600 Å³ (Figure S9).^[16] A two-fold crystallographic

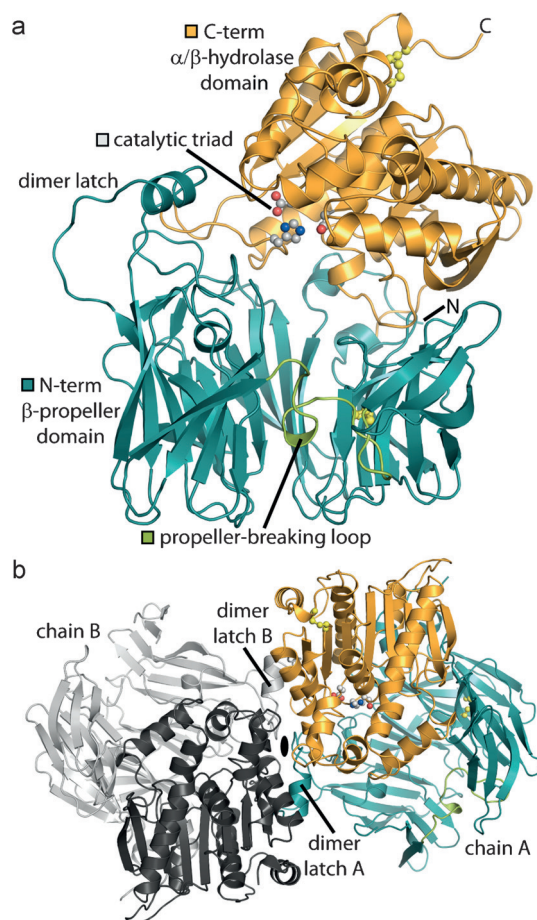


Figure 5. The architecture of Spl-IsoP. a) Front view of chain A of SeMet-derived Spl-IsoP (PDB ID: 5JRK). The side chains of catalytic triad residues (S559, H671, D582) and disulfide bonds (yellow) are shown. b) The Spl-IsoP homodimer, viewed along the two-fold symmetry axis (black ellipse). Chain A is colored as in (a); chain B is colored by domain in shades of gray.

dimer interface of approximately 4860 Å² is buried^[17] between one side of each chain (Figure 5b and Figure S10). Gel-filtration analysis supports a dimeric state for the enzyme in solution (Figure S11).

The N-terminal domain of the IsoP is comprised of a broken seven-bladed β -propeller, wherein each blade is generally constructed of four twisted, antiparallel β -strands (Figure S12). However, blade 5, which follows a flexible, propeller-breaking loop (residues 277–292), lacks one β -strand (Figure 5 and Figure S13). These features are presumably important for entry of the bulky lasso peptide substrate. As is typical of β -propeller domains, the blades of SpI-IsoP are held together largely by hydrophobic interactions and are radially arranged with a pore extending through the center.^[18]

A short hinge connects the last strand of the β -propeller to the C-terminal α/β -hydrolase domain (Figure S14). The latter harbors a catalytic triad (S559-H671-D582) characteristic of serine proteases, wherein a proton relay network facilitates deprotonation of the nucleophile, S559 (Figure 6).^[8] Conformational changes may enhance this network, as reported for a POP that was crystallized in open and closed states.^[19] A

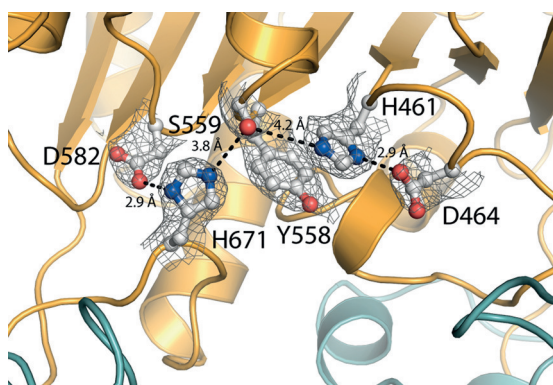


Figure 6. A magnified view of the active site of SpI-IsoP. Distances between potential hydrogen-bond donors and acceptors are labeled (dashed lines). A $2F_o - F_c$ density map is shown at 1.0σ .

helix dipole likely further promotes deprotonation of S559. While S559 and H671 are fully conserved among IsoPs, D582 is normally found at an alternate position (Figure S15). On the opposite side of S559 resides H461 (conserved as H/Y), which, in addition to the backbone NH of R560, likely stabilizes the negative charge of the oxyanion intermediate.^[8] The side chain of Y558 is π -stacked between W476 and H461 and makes van der Waals contact with S559 and H671—it may, therefore, properly position the catalytic residues.

In order to clarify the roles of the aforementioned residues in isopeptide bond cleavage, we prepared a set of SpI-IsoP variants (Figure S2a–p). Each variant was incubated with SpI for 1, 5, 30, or 60 min at 30 °C, then quenched and analyzed (under these conditions, wt SpI-IsoP fully hydrolyzes the given amount of SpI within 5 min). As expected, the catalytic-triad variants H671A and H671Q were inactive, which verifies the crucial role of H671 in deprotonating the nucleophilic S559 and water. The inactivity of variant S559C may indicate that the bulkier thiol group disrupts the proton relay network, while the trace activity observed for variant S559A suggests that, in the absence of steric hindrance, hydrolysis can still be catalyzed (albeit slowly) without the formation of a covalent intermediate. Substitution of D582 with Ala or Asn resulted in moderate or trace conversion, respectively, thus implying that a catalytic diad is sufficient for hydrolysis. Exchange of the nonconserved D464 with Ala or Asn resulted in trace or minor conversion, respectively, thus suggesting that this residue aids in positioning H461 through H-bonding. No, trace, minor, or moderate conversion was observed for variants H461Q, H461A, H461Y, or H461N, thus indicating that various side chains can stabilize the tetrahedral intermediate, but with altered efficiency that may depend on steric, H-bonding, hydrophobic, and/or ionization character. While no or trace conversion was detected for variants Y558I and Y558A, respectively, variant Y558F displayed good conversion, which supports the proposed steric influence of the aromatic side chain in positioning S559, H461, and H671. Additionally, we measured reaction rates for the most active variants D464N, D582A, and Y558F in comparison to wt SpI-IsoP. Much higher concentrations of these variants were needed to achieve comparable conversion, thus further

highlighting the finely tuned nature of the SpI-IsoP active site (Figure S16).

To investigate whether a patch of basic residues on SpI-IsoP aids in binding the acidic SpI, variants were prepared and assayed as above (Figures S2q–t and S17a). Indeed, variant R228A cleaved only minor amounts of SpI, and the variants R232A and R232A/R236A showed a moderate reduction in activity, although structural roles cannot be excluded for these residues. Notably, variant R236A was as active as the wt enzyme. Attempts to align counter-charged residues or place the isopeptide bond of SpI near S559 of SpI-IsoP resulted in serious clashes, thus indicating that major conformational changes are necessary. Motions that bring the two domains of SpI-IsoP closer together or farther apart are hypothesized based on existing structures of POPs (Figure S18).^[19,20] Such motions could allow access of the substrate to the binding pocket, followed by trapping and hydrolysis. Future molecular dynamics or cocrystallization studies may unveil the specifics of the interaction.

In conclusion, we report the first structure of a lasso peptide isopeptidase (SpI-IsoP), which represents a new class of POP-like serine proteases. Such proteases are the only known enzymes whose sole function is to catabolize RiPPs.^[9] Structure-guided mutational analysis allowed us to propose which active-site residues comprise the catalytic triad and oxyanion hole. We also report the structure of SpI, confirming its lasso fold. Failure of the IsoP to hydrolyze a diverse panel of lasso peptides suggests strict specificity toward threaded SpI, its native substrate. However, single-residue variants of SpI were still hydrolyzed by SpI-IsoP, thus indicating that the enzyme tolerates subtle changes and likely recognizes multiple topology-conferring features. Future studies will be required to clarify the exact nature of the recognition, as well as the biological function of SpI and the necessity for such a large, dedicated protease. We hypothesize that the lasso peptide functions as a signal molecule that is imported by the TonB-dependent receptor, propagated as a signal by the σ /*anti*- σ factors, and subsequently linearized by the IsoP.

Acknowledgements

We gratefully acknowledge the Deutsche Forschungsgemeinschaft and SYNMIKRO (Hessen) for financial support. We thank the European Synchrotron Radiation Facility (Grenoble, France) and the MarXtal Facility (Marburg) for support with crystallographic experiments. We thank Julian Koch, Sabrina Henche, Levke Anderson, Bastian Langer, Jessica Pilgram, Henrik Müller and Antje Schäfer for technical assistance, and Andreas Heine and Pavel Afonine for helpful discussions.

Keywords: hydrolases · isopeptidases · lasso peptides · natural products · protein structures

How to cite: *Angew. Chem. Int. Ed.* **2016**, *55*, 12717–12721
Angew. Chem. **2016**, *128*, 12909–12913

- [1] a) J. D. Hegemann, M. Zimmermann, X. Xie, M. A. Marahiel, *Acc. Chem. Res.* **2015**, *48*, 1909–1919; b) M. O. Maksimov, A. J. Link, *J. Ind. Microbiol. Biotechnol.* **2014**, *41*, 333–344.
- [2] a) J. D. Hegemann, C. D. Fage, S. Zhu, K. Harms, F. S. Di Leva, E. Novellino, L. Marinelli, M. A. Marahiel, *Mol. Biosyst.* **2016**, *12*, 1106–1109; b) M. O. Maksimov, A. J. Link, *J. Am. Chem. Soc.* **2013**, *135*, 12038–12047.
- [3] J. D. Hegemann, M. De Simone, M. Zimmermann, T. A. Knappe, X. Xie, F. S. Di Leva, L. Marinelli, E. Novellino, S. Zahler, H. Kessler, M. A. Marahiel, *J. Med. Chem.* **2014**, *57*, 5829–5834.
- [4] a) S. S. Elsayed, F. Trusch, H. Deng, A. Raab, I. Prokes, K. Busarakam, J. A. Asenjo, B. A. Andrews, P. van West, A. T. Bull, M. Goodfellow, Y. Yi, R. Ebel, M. Jaspars, M. E. Rateb, *J. Org. Chem.* **2015**, *80*, 10252–10260; b) E. Gavriš, C. S. Sit, S. Cao, O. Kandror, A. Spoering, A. Peoples, L. Ling, A. Fetterman, D. Hughes, A. Bissell, H. Torrey, T. Akopian, A. Mueller, S. Epstein, A. Goldberg, J. Clardy, K. Lewis, *Chem. Biol.* **2014**, *21*, 509–518; c) Y. Li, R. Ducasse, S. Zirah, A. Blond, C. Goulard, E. Lescop, C. Giraud, A. Hartke, E. Guittet, J. L. Pernodet, S. Rebuffat, *ACS Chem. Biol.* **2015**, *10*, 2641–2649; d) M. Metelev, J. I. Tietz, J. O. Melby, P. M. Blair, L. Zhu, I. Livnat, K. Severinov, D. A. Mitchell, *Chem. Biol.* **2015**, *22*, 241–250; e) V. Valiante, M. C. Monteiro, J. Martin, R. Altwasser, N. El Aouad, I. Gonzalez, O. Kniemeyer, E. Mellado, S. Palomo, N. de Pedro, I. Perez-Victoria, J. R. Tormo, F. Vicente, F. Reyes, O. Genilloud, A. A. Brakhage, *Antimicrob. Agents Chemother.* **2015**, *59*, 5145–5153.
- [5] a) B. J. Burkhart, G. A. Hudson, K. L. Dunbar, D. A. Mitchell, *Nat. Chem. Biol.* **2015**, *11*, 564–570; b) K. P. Yan, Y. Li, S. Zirah, C. Goulard, T. A. Knappe, M. A. Marahiel, S. Rebuffat, *ChemBioChem* **2012**, *13*, 1046–1052.
- [6] a) M. O. Maksimov, I. Pelczer, A. J. Link, *Proc. Natl. Acad. Sci. USA* **2012**, *109*, 15223–15228; b) H. G. Choudhury, Z. Tong, I. Mathavan, Y. Li, S. Iwata, S. Zirah, S. Rebuffat, H. W. van Veen, K. Beis, *Proc. Natl. Acad. Sci. USA* **2014**, *111*, 9145–9150.
- [7] a) J. D. Hegemann, M. Zimmermann, X. Xie, M. A. Marahiel, *J. Am. Chem. Soc.* **2013**, *135*, 210–222; b) J. D. Hegemann, M. Zimmermann, S. Zhu, H. Steuber, K. Harms, X. Xie, M. A. Marahiel, *Angew. Chem. Int. Ed.* **2014**, *53*, 2230–2234; *Angew. Chem.* **2014**, *126*, 2262–2266; c) J. D. Hegemann, M. Zimmermann, S. Zhu, D. Klug, M. A. Marahiel, *Biopolymers* **2013**, *100*, 527–542; d) M. Zimmermann, J. D. Hegemann, X. Xie, M. A. Marahiel, *Chem. Sci.* **2014**, *5*, 4032–4043.
- [8] a) V. Fülöp, Z. Böcskei, L. Polgár, *Cell* **1998**, *94*, 161–170; b) V. Fülöp, Z. Szeltner, L. Polgár, *EMBO Rep.* **2000**, *1*, 277–281; c) L. Polgár, *Cell. Mol. Life Sci.* **2002**, *59*, 349–362.
- [9] M. O. Maksimov, J. D. Koos, C. Zong, B. Lisko, A. J. Link, *J. Biol. Chem.* **2015**, *290*, 30806–30812.
- [10] S. M. Nijman, M. P. Luna-Vargas, A. Velds, T. R. Brummelkamp, A. M. Dirac, T. K. Sixma, R. Bernards, *Cell* **2005**, *123*, 773–786.
- [11] E. T. Yeh, *J. Biol. Chem.* **2009**, *284*, 8223–8227.
- [12] K. Kanchan, E. Ergulen, R. Kiraly, Z. Simon-Vecsei, M. Fuxreiter, L. Fesus, *Biochem. J.* **2013**, *455*, 261–272.
- [13] K. Takeshita, Y. Hashimoto, T. Ueda, T. Imoto, *Cell. Mol. Life Sci.* **2003**, *60*, 1944–1951.
- [14] a) M. Zimmermann, J. D. Hegemann, X. Xie, M. A. Marahiel, *Chem. Biol.* **2013**, *20*, 558–569; b) M. Tsunakawa, S. L. Hu, Y. Hoshino, D. J. Detlefson, S. E. Hill, T. Furumai, R. J. White, M. Nishio, K. Kawano, S. Yamamoto, Y. Fukagawa, T. Oki, *J. Antibiot.* **1995**, *48*, 433–434; c) W. Weber, W. Fischli, E. Hochuli, E. Kupfer, E. K. Weibel, *J. Antibiot.* **1991**, *44*, 164–171; d) T. A. Knappe, U. Linne, X. Xie, M. A. Marahiel, *FEBS Lett.* **2010**, *584*, 785–789; e) T. A. Knappe, U. Linne, S. Zirah, S. Rebuffat, X. Xie, M. A. Marahiel, *J. Am. Chem. Soc.* **2008**, *130*, 11446–11454.
- [15] T. A. Knappe, U. Linne, L. Robbel, M. A. Marahiel, *Chem. Biol.* **2009**, *16*, 1290–1298.
- [16] N. R. Voss, M. Gerstein, *Nucleic Acids Res.* **2010**, *38*, W555–562.
- [17] E. Krissinel, K. Henrick, *J. Mol. Biol.* **2007**, *372*, 774–797.
- [18] C. K. Chen, N. L. Chan, A. H. Wang, *Trends Biochem. Sci.* **2011**, *36*, 553–561.
- [19] P. Canning, D. Rea, R. E. Morty, V. Fülöp, *PLOS ONE* **2013**, *8*, e79349.
- [20] a) L. Shan, I. I. Mathews, C. Khosla, *Proc. Natl. Acad. Sci. USA* **2005**, *102*, 3599–3604; b) M. Li, C. Chen, D. R. Davies, T. K. Chiu, *J. Biol. Chem.* **2010**, *285*, 21487–21495.

Received: May 29, 2016

Revised: July 21, 2016

Published online: September 9, 2016